



SEISMOLOGY

Estimating shear wave velocity using acceleration data in Antakya (Turkey)

Aydın Büyüksaraç¹, Semir Över², M. Cemal Genç³, Murat Bıkçe⁴, Selçuk Kaçın⁴, Özcan Bektaş⁵

1. Bitlis Eren University, Civil Engineering Dept., TR-13000 Bitlis-Turkey

2. Mustafa Kemal University, Geophysical Engineering Dept. TR-31200 Iskederun/Antakya- Turkey

3. Zirve University, Civil Engineering Dept. TR-27260 Gaziantep- Turkey

4. Mustafa Kemal University, Civil Engineering Dept. TR-31200 Iskederun/Antakya- Turkey

5. Cumhuriyet University, Geophysical Engineering Dept. TR-58140 Sivas- Turkey

Correspondence author: Aydın Büyüksaraç. E-mail: absarac@comu.edu.tr

ABSTRACT

This manuscript presents a site response analysis and an estimation of S-wave velocity that are dependent on acceleration data. First, existing data, such as density, seismic wave velocity, and soil cross-sections, are obtained from previous seismic microzonation studies and used to prepare input data for a suite of MATLAB routines, which are referred to as SUA software. Acceleration data are obtained from four free-field strong-motion stations of the SERAMAR project, which was conducted between 2006 and 2009 in conjunction with a Turkish-German joint research project, and inputted into the software as basic data. The results include a 1D velocity cross-section versus depth and an amplification model of the site. Three different depth levels can be determined for the ranges of 0-5 m, 5-15 m and 15-25 m. The seismic velocities vary between 380 and 470 m s⁻¹ for the first 5 m; 320 and 480 m s⁻¹ for 5-15 m; and 470 and 750 m s⁻¹ for 15-25 m. These results are comparable with the amplification values from the microtremor data from previous studies. The 1D velocity models are appropriate for the soil conditions.

Key Words: Acceleration data, shear wave velocity, Antakya, soil conditions, 1D velocity model.

RESUMEN

Este trabajo presenta el análisis a una respuesta de sitio y una estimación de la velocidad de la onda de corte que son dependientes de la información de aceleración. Los datos adicionales como la densidad, la velocidad de onda sísmica y los cortes transversales de suelo, se obtuvieron de estudios previos de microzonificación sísmica y se utilizaron para preparar el registro de datos en una plataforma de rutinas MATLAB, que se refieren al software SUA. Los datos de información de la aceleración se tomaron de cuatro estaciones de monitoreo de movimientos fuertes a campo abierto del proyecto SERAMAR, que se realizó entre 2006 y 2009 en una investigación conjunta turco-alemana, y se ingresaron en el programa como la información básica. Los resultados incluyen una sección cruzada de velocidad 1D versus profundidad y el modelo amplificado del sitio. Se pudieron determinar tres niveles diferentes a partir de los rangos de 0-5 m, 5-15 m y 15-25 m. Las velocidades sísmicas pueden variar entre 380 y 470 m s⁻¹ para los primeros 5 metros; 320 y 480 m s⁻¹ para el rango 5-15 m, y 450 y 750 m s⁻¹ para el rango 15-25 m. Estos resultados son comparables con los valores de amplificación del perfil Microtemor de estudios previos. Los modelos de velocidad 1D son apropiados para las condiciones del suelo.

Palabras clave: Información de aceleración; ondas de corte; Antakya; condiciones de suelo, modelos de velocidad 1D.

Record

Manuscript received: 30/01/2014
Accepted for publication: 23/09/2014

Introduction

Site characteristics of urban areas are primarily estimated by analyses of recorded ground motions. The estimation of site characterization is very important for disaster mitigation planning. However, the types of recorded ground motions differ. Because large- or moderate-sized earthquakes do not occur on a frequent basis, they cannot be considered as a source of ground motion. In this case, the site characteristics may be estimated from microtremors or small-sized frequent earthquakes (Shrikhande and Basu, 2004), which are divided into zones according to their similarities after estimation of the site characteristics. This process is referred to as microzonation. Microzonation establishes several parameters that are associated with disasters such as earthquakes and landslides. However, microzonation provides a detailed description of earthquake hazards for the selected locality in a seismic microzone. This process is known as seismic microzonation. Data from seismic microzonation includes the intensity of shaking at the bedrock level, the site characteristics, the predominant period and the spectral amplification of surface motion with respect to bedrock motion (Shrikhande and Basu, 2004). The distribution of damage caused by earthquake ground shaking commonly reflects regional areal differences in local soil conditions. Earthquake damage is significantly greater on thick deposits of unconsolidated sediments compared with nearby bedrock locations. As a result, the site conditions should be considered as part of the assessment of ground motion hazards. Studies indicate that shear-wave velocity is a critical factor in determining the intensity of ground shaking and is a useful parameter for characterizing local soil conditions in ground motion studies (Over *et al.*, 2011).

The behavior of soil layers at large strains associated with strong earthquakes is normally nonlinear; therefore, it should be considered in seismic microzonation studies. The majority of researchers currently prefer to use microtremor measurements to estimate seismic microzonation maps. However, to estimate site characteristics from microtremors or weak motion data, all techniques are based on linear system theory (Shrikhande and Basu, 2004). Microtremors have been used to estimate the resonant period of a site since 1957; the results were used to specify the earthquake design forces in various zones in Japan depending on the predominant period (Kanai, 1957). The characteristics of microtremors were compared with strong earthquake accelerograms recorded in El Centro, California by Udvardi and Trifunac (1973). They concluded that the characteristics of microtremors significantly differ from the characteristics of strong earthquake accelerograms. Many researchers have investigated ground motion behavior to establish a correlation between average shear wave velocity and the site amplification factors. Surface wave recordings are very useful for seismic response analyses of the sites. This approach is very important to understand the behavior of soils because the soil conditions are related to the mechanical characteristics of surface soils, such as the slope of the soils, and the depth of the ground water table. The estimation of these conditions, which are related to the soils, increases the cost of the site investigations. The soil behavior during earthquakes or microtremors reflects its conditions. Seismic hazard analysis provides a framework for which uncertainty in the size, location and likelihood of future earthquakes can be incorporated to model earthquake hazard.

In this paper, a simple approach was applied to estimate the level of uncertainty in the modelled amplification factors due to variations in alluvial thickness and velocity structure. MATLAB routines, which are referred to as SUA, are provided to implement an equivalent linear site-response analysis with the option of an assessment of uncertainty (Robinson *et al.*, 2006). The presence of soils, geological sediments and weathered rocks can amplify the level of ground shaking experienced during an earthquake. Consequently, the effect of the type of soil on earthquake ground shaking is an important component for a seismic hazard analysis. This paper provides a detailed and comprehensive description of an equivalent linear site-response analysis, which is a technique for modelling the amplification of seismic waves due to propagation through alluvial soil in Antakya. The description includes a theoretical solution for the wave equation, derivation of a transfer function that relates bedrock acceleration to surface acceleration, calculation of a response spectral acceleration and computation of an amplification factor.

1. Overview of the Geology, Seismicity and Soil Conditions of Antakya

In the eastern Mediterranean, plate motions occur between the Arabia/Anatolia, Africa/Arabia and Anatolia/Africa boundaries along the left lateral Amanos Fault, the Dead Sea Fault and the Cyprus Arc, and the extension of the latter on land [named the Cyprus-Antakya Transform Fault by Over *et al.* (2004a)]. Active faults that are associated with the previously mentioned structural zones join to form a triple junction at the Quaternary Amik Basin near Antakya (Over *et al.*, 2004a). The seismicity and filling of the quaternary age in Antakya and its surrounding area have been controlled by these active major faults.

The length of the NNE-trending segment is approximately 145 km and is known as the Amanos Fault (Lyberis *et al.*, 1992) or Karasu Fault (Westaway, 1994), which has been considered to be a southern continuation of the East Anatolian Fault Zone (EAFZ) (Over *et al.*, 2002; Over *et al.*, 2004a). It is located along the western flanks of the Karasu Valley and the Amik basin, which has a width of approximately 30 km, and is filled with Plio-Quaternary sediments to create a thickness greater than 1000 m (Perincek and Eren, 1990). Some isotopic dating studies suggest a Quaternary to recent age for the basaltic rocks along the Karasu Valley (Rojay *et al.*, 2001). Plio-Quaternary sediments and Quaternary volcanics unconformably overlie Miocene beds (Fig. 1).

Several authors (Ergin *et al.*, 1967; Ambraseys, 1970; McKenzie, 1972, 1978; Soysal *et al.*, 1981; Rotstein and Kafka, 1982) have described the general trends of seismicity in the eastern Mediterranean, Anatolia and Levant countries. During this century, this region has been characterized by a low seismicity (Jackson and McKenzie, 1988). However, it is known to have been seismically active based on historical catalogues (Poirier and Taher, 1980; Ambraseys and Barazangi, 1989). Two large historical earthquakes (denoted by stars in Fig. 2) destroyed the town of Antakya on August 13, 1822 ($M_s=7.4$) and April 13, 1872 ($M_s=7.2$) (Ergin *et al.*, 1967), which caused more than 20,000 deaths in the region (Kalafat and Bagci, 2001). These historical events caused surface ruptures with lengths of 20 km and 30 km along directions of $N30^\circ$ and $N20^\circ E$, respectively (Ambraseys and Jackson, 1998).

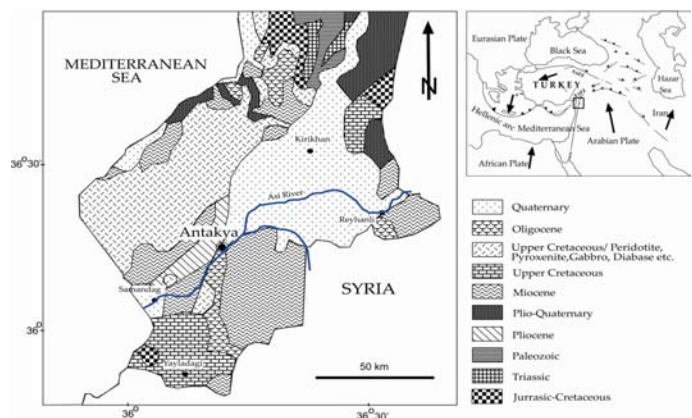


Figure 1: Geological map of Antakya. Inset map shows the location and main tectonic units. NAFZ: North Anatolian Fault Zone, EAFZ: East Anatolian Fault Zone (Over *et al.*, 2011).

The most important earthquake during the instrumental period occurred on January 22, 1997; it had a body-wave magnitude (M_b) of 5.5 and aftershocks with M_b of 5.2 and 5.3 and maximum intensity of $I_0=VI-VII$, which caused damage in certain buildings (Erdik *et al.*, 1997).

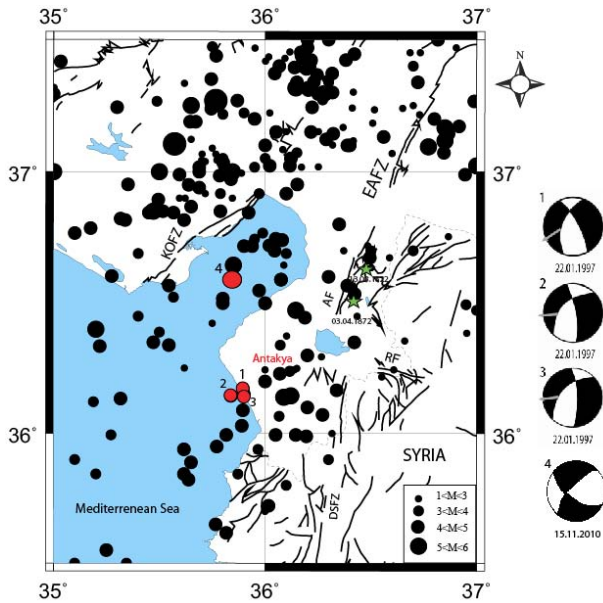


Figure 2: Seismicity and seismotectonic map of the Hatay region and surroundings, and some focal mechanisms of shallow earthquakes. The red points represent the earthquakes in 1997. EAFZ: East Anatolian Fault Zone, DSFZ: Dead Sea Fault Zone, KOFZ: Karataş Osmaniye Fault Zone, RF: Reyhanli Fault, and AF: Amanos Fault.

Data on the near-surface geological conditions are important for understanding the site amplifications that were experimentally measured using the earthquakes. Two deep borehole logs provide a vertical profile of the surface deposits up to 60 m (W1) and 100 m (W2), respectively (Table 1). Antakya Municipality housing is situated along the two sides of the Asi River, which originates in Syria and runs to the Mediterranean Sea through Antakya city. The sediments within the Antakya region are primarily composed of Quaternary alluvial fill, which consists of clay, silt, sand and gravel. The soil description in the borehole logs show that the surface soil consists of quaternary materials composed of clay, gravel detritic formations of conglomerates and alluvial sands. The average ground water level in the area is 3 m according to the deep boreholes.

Table 1: Deep boreholes in the study area (W1=60 m and W2=100 m) (Over et al., 2008)

W1		W2	
Depth (m)	Formation	Depth (m)	Formation
0 - 1	Agricultural Soil table	0 - 7	Gravel with clay
1 - 7	Gravel	7 - 26	Clay
7 - 11	Clay stone	26 - 36	Gravel
11 - 18	Clay Stone with Gravel	36 - 76	Clay
18 - 22	Gravel	76 - 80	Gravel
22 - 26	Conglomerate	80 - 90	Clay
26 - 29	Conglomerate with Clay	90 - 100	Gravel with Clay
29 - 33	Conglomerate		
33 - 53	Conglomerate with Clay		
53 - 60	Clay Stone		

2. Site Effects from H/V Ratios and Vs30 Analysis

The fundamental frequencies of the near-surface deposits at a site are a valuable tool for developing land-use plans for urban regions that consider earthquake disaster mitigation. Here, the resonant periods and site amplifications are determined by dividing the smoothed Fourier amplitude spectrum of the horizontal component by the smoothed spectrum of the vertical component that was recorded at the same site, which eliminates the need for a reference site. The spectral ratio technique for estimating the transfer function for the site response, involves the ratio of the Fourier amplitude spectrum of the motion recorded at the site to the Fourier amplitude spectrum of the same motion recorded at a nearby reference site, has been proposed to estimate the resonant periods of the site (EDAC, 2004).

Over et al. (2011) analyzed the microtremor data for Antakya. The H/V spectra were obtained for all observation sites, and the predominant periods of all sites were identified. The microtremor measurements show that the predominant period for the sites in Antakya range from approximately 0.2 s to 0.8 s (Fig. 3).

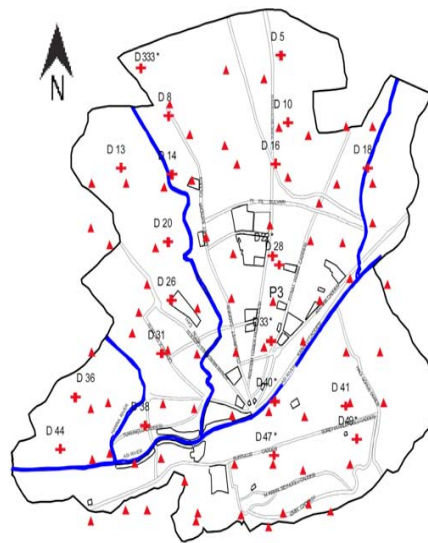


Figure 3: Locations of sections from combination of microtremor and ReMi measurement positions. ▲ represents microtremor observations and ✚ represents ReMi observations.

3. Data

3.1. Strong-motion stations

In close collaboration with Mustafa Kemal University (MKU) and other local partners, the Earthquake Damage Analysis Center (EDAC) at Bauhaus-Universität Weimar initiated a Turkish-German joint research project on Seismic Risk Assessment and Mitigation in the Antakya-Maras-Region (SERAMAR) (EDAC 2004). In the framework of the SERAMAR Project, three reinforced concrete structures were equipped with a building monitoring system manufactured by SYSCOM Instruments of Switzerland. In this building monitoring system, three or four sensors were installed on the structure and one sensor was installed on the free field (Schwarz et al., 2007). The sensors were MR2002+ triaxial accelerometers with a linear 0 to 150 Hz frequency response range and a ± 2 g measuring range. The free-field station was installed at a distance that was equivalent to the minimum height of one instrumented or neighboring building (Schwarz et al., 2007). Data obtained from the fourth station, which were instrumented by the General Directory of Disaster Affairs of Turkey, were employed in this study (Fig. 4). The instruments consisted of Kinematics Etna with three channels and an internal triaxial EpiSensor Force Balance Accelerometer.

3.2. Acceleration data

In the considered time-window between 2006 and 2009, approximately 30 earthquakes were recorded and identified at these stations (Abrahamczyk *et al.*, 2008; Schwarz *et al.*, 2009). All earthquake parameters were derived from the website of the Kandilli Observatory and the Earthquake Research Institute (KOERI) Bulletins, as shown in Table 2.



Figure 4: Locations of accelerometer stations: stations I, II and III are free-field stations of the building monitoring systems, whereas station IV is an independent free-field station.

Table 2: List of the measured earthquakes in the project area.

No.	Date	Location		h (km)	Md	MI	Recorder			
		Lat.	Long.				Sta-II	Sta-I	Sta-III	Sta-IV
1	19/09/2006	35.95	35.77	22	3.8			•	•	•
2	09/10/2006	35.82	35.60	39	4.3		•	•	•	•
3	07/01/2007	37.13	36.09	20	3.9		•			
4	25/01/2007	36.12	35.90	17	3.0		•	•		
5	01/02/2007	35.84	35.90	12	3.6		•	•	•	
6	03/02/2007	36.95	35.42	27	3.6		•	•		
7	11/03/2007	36.56	35.88	6	3.8			•		
8	14/03/2007	36.47	35.86	4	3.2			•		
9	12/05/2007	36.39	35.63	8	3.8		•	•		
10	15/05/2007	35.97	35.83	5	3.1		•			
11	21.01.2008	37.00	36.12	7.0	2.9		•	•		
12	07.03.2008	36.78	36.42	8.7	3.2		•			•
13	10/03/2008	36.61	36.47	6.8	2.8			•		•
14	17/04/2008	36.28	36.13	7.3	3.3		•	•		•
15	03/05/2008	36.73	36.62	7.1	3.9		•			
16	12/06/2008	36.25	36.06	7.4	3.0		•			•
17	19/06/2008	36.63	36.05	6.8	3.7					•
18	01/11/2008	36.06	35.86	24.2	3.3					•
20	18/11/2008	36.22	36.98	7.0	2.9	-	•			•
21	30/11/2008	36.24	36.11	7.0	2.7	-	•			•
22	04/12/2008	36.18	36.02	7.2	2.9	-	•			
23	10/12/2008	36.04	36.25	8.4	3.2	-	•			
24	19/12/2008	36.21	36.29	7.0	3.0	-	•			
25	19/12/2008	35.93	36.36	7.0	2.8	-				•
26	17/01/2009	37.16	36.31	7.5	-	4.6		•		•
27	22/01/2009	36.11	35.88	24.6	3.4	-		•		•
28	22/01/2009	36.09	35.83	22.8	3.1	-		•		•
29	05/02/2009	36.20	36.09	7.4	3.1	-	•			•
30	09/02/2009	36.09	36.05	2.1	3.3	-				•

The magnitudes of the earthquakes (Md) ranged from 2.7 - 4.3. A total of 30 acceleration data were obtained from the time histories of this area. Several earthquakes with magnitudes (Md) that ranged from 3.0 - 4.3 were measured. Examples of recorded acceleration time histories are given in Figure 5 (Schwarz *et al.*, 2007). The response spectrum is the most suitable tool for expressing the excitation response relation in earthquake engineering and seismic design. Although it is an indirect measure of ground intensity, it directly expresses the maximum response, which is a major concern in structural design. If sets of response spectra for ground motions recorded at different locations during previous earthquakes are generated, a large variation would be observed in both the response spectral values and the shape of the spectra will vary among the sets.

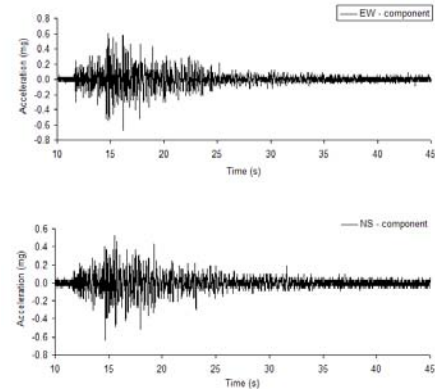


Figure 5: Recorded building response due to a magnitude ML = 3.1 earthquake (March 3, 2008); sensor: free-field of the building (a) Recorded acceleration time histories.

These variations are dependent on many factors, such as the energy release mechanism in the vicinity of the focus or the hypocenter and along the fault interfaces, the epicentral distance and the focal depth, the geology and its variations, the energy transmission paths, the Richter magnitude and the local soil conditions at the recording station. Thus, the response spectral values S (S_p , S_a and S_d) (Eq. 1) for earthquake ground motion should be considered to be a function expressed in the following form (Clough and Penzien, 1993; Tehranizadeh and Hamed, 2002)

$$S = S(SM, ED, FD, GC, M, SC, \xi, T) \quad (1)$$

$$S = S(SC, \xi) \quad (2)$$

where the independent variables include SM: source mechanism, ED: epicentral distance, FD: focal depth, GC: geological conditions, M: Richter magnitude, SC: soil conditions, ξ : damping ratio and T: period. The effects of SM and GC on both the spectral values and the shapes of the response spectra are not well understood; therefore, these effects cannot be quantified when defining response spectra for design purposes. The effects of ED, FD and M are usually considered when specifying the intensity levels of the design response spectra; however, they are frequently disregarded during the specification of the shape of these spectra due to a lack of knowledge regarding their influences. The effect of SC on both the intensities and the shapes of the response spectra are considered in the definition of the design response spectra (Tehranizadeh and Hamed, 2002).

In many cases, the ratio of the spectral acceleration to the peak ground acceleration (acceleration amplification) is plotted as a function of either frequency or period (Mohraz and Elghadamsi, 1989). Studies have shown that the response spectra from accelerograms recorded on similar soil conditions reflect similarities in shape and amplification. For this reason, the response spectra from records with common characteristics are averaged and smoothed before they are used in design (Mohraz and Elghadamsi, 1989).

4. Antakya Case Study

Robinson et al. (2006) collectively described the presence of soils, geological sediments and weathered rock as regolith and developed MATLAB routines, which are referred to as SUA, to model the amplification of seismic waves due to propagation through regolith from Sydney, Australia.

Antakya exhibits high risk due to earthquakes. The approach of Robinson et al. (2006) was employed with available geotechnical information to investigate the potential for ground motion amplification in Antakya. Antakya is located within the Amik Basin, which comprises a sequence of Plio-Quaternary sediments with a minimum thickness of 1000 m from a variety of geological environments, including sand, gravel, clay and silt. Five site classes were identified in Antakya using microtremor data and seismic velocities obtained by Over *et al.* (2011).

The surface acceleration time history and the response spectral acceleration for the recorded earthquakes in the stations (Table 2) were obtained using SUA software (Robinson et al., 2006). The methodology

enabled a broad-scale site-response analysis despite limited geotechnical data. The analysis provided an indication of the level of uncertainty associated with the two geotechnical parameters layer thickness and seismic velocity, for which the amplification factors are the most sensitive. The SUA software packages are designed for individual site-response analysis and do not define the site response for a larger region.

Accelerometers were installed in two different soil types to record multiple earthquake data in the framework of the SERAMER Project. We prepared input data for SUA software for each of the four locations using Vs data on the densities of shallow wells drilled by private firms. One-dimensional velocity versus depth was calculated for all four locations by controlling the acceleration data for each station (Figures 6a, b, c, d). The cross-sections were simulated from the site classes using the approach suggested by Robinson et al. (2006) to produce amplification factors for acceleration time history combinations.

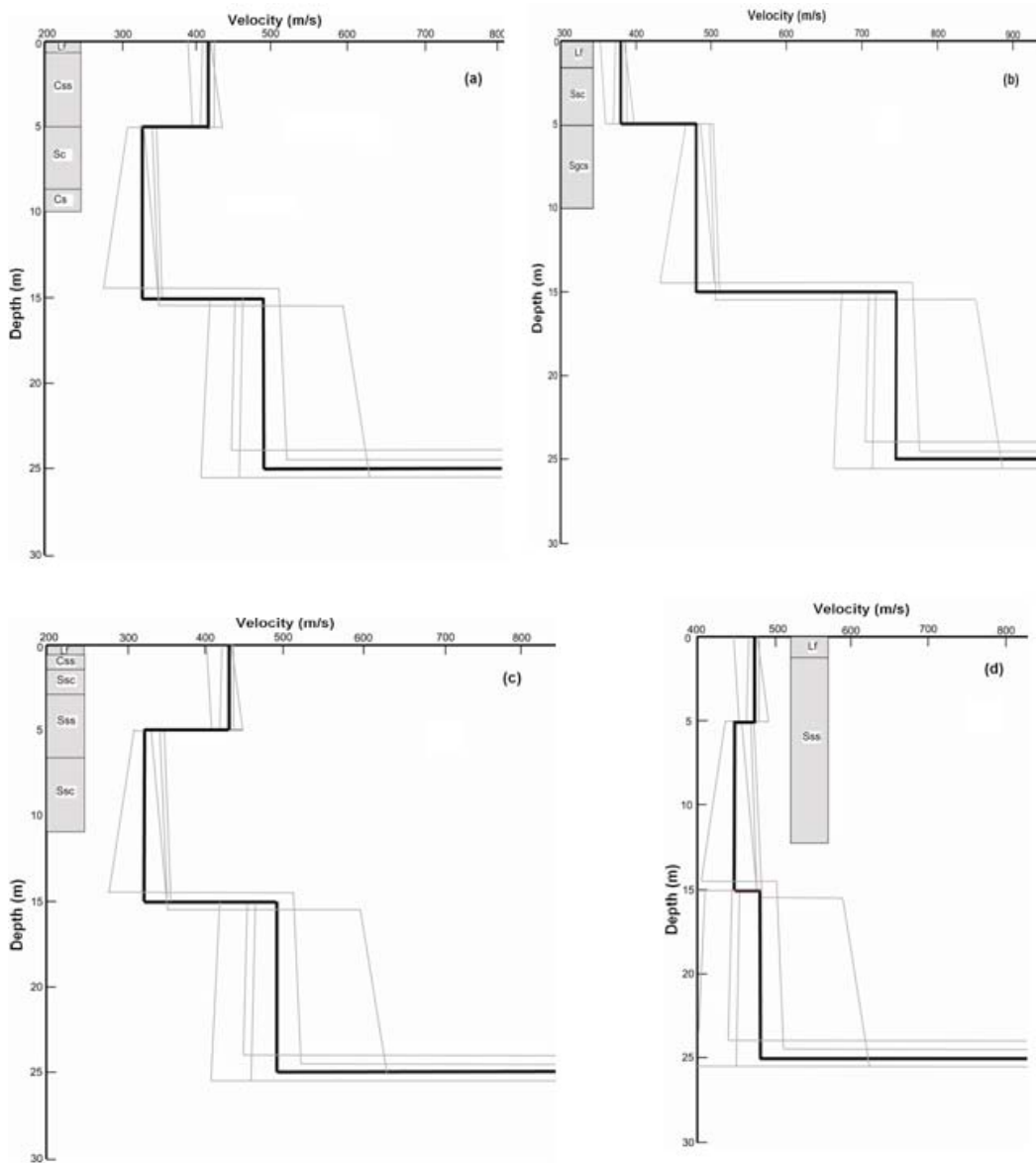


Figure 6: 1-D Velocity models generated from acceleration data using input data site class 4 for Station I and site class 2 for stations II, III and IV. (a) Station I, (b) Station II, (c) Station III, and (d) Station IV. Gray colored drilling logs show the soil condition at the station. Lf: Landfill, Ccs: Clay with silt and sand, Ssc: Silt with sand and clay, Sss: Sand with silt and sand, Sgcs: Sand with gravel, clay and silt, Gcs: Gravel with clay and sand, Sc: Sand with clay, and Cs: Clay with sand.

Amplification factors are assumed to be log-normally distributed. Note that the mean in log-space is equivalent to the median in normal space. The median amplification factors are shown within the 16th and 84th percentiles in Figures 7a, b, c, d.

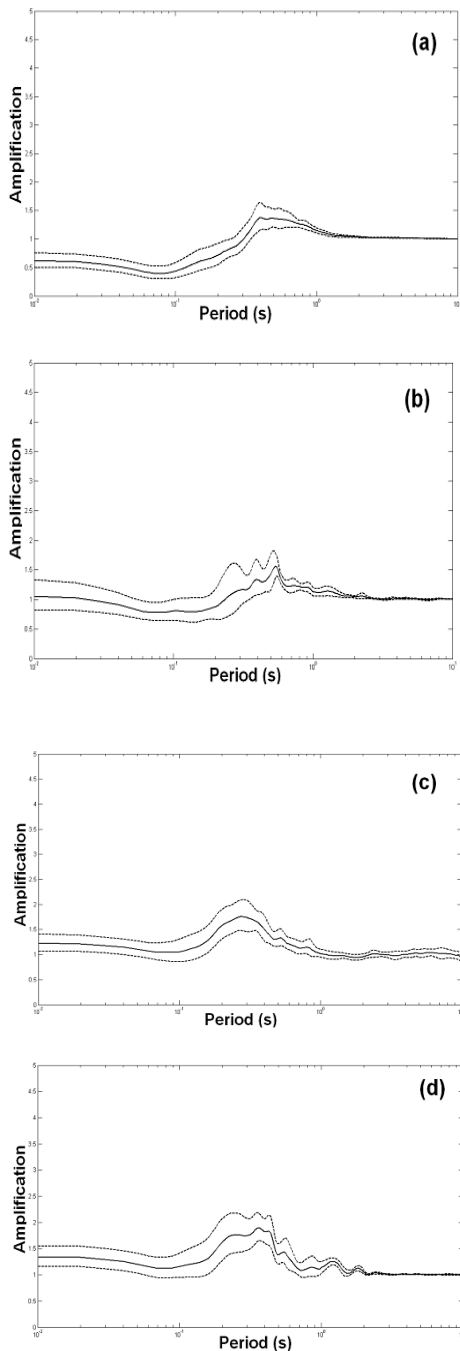


Figure 7: Median amplification factor (solid line) and 16th and 84th percentiles (dashed lines) (a) Station I, (b) Station II, (c) Station III, and (d) Station IV.

5. Discussion and Conclusions

This paper describes the site response and velocity changes using acceleration data with inversion for four acceleration stations in Antakya. The study also uses the microzonation results of Over *et al.* (2011).

1 - The median amplification factor indicated the following maximum levels of amplification: 1.5 at 0.4 s periods for Station I, 1.5 at 0.5 s periods for Station II, 2 at approximately 0.25 s periods for Station III, and 2 at 0.4 s periods for Station IV, which approximately corresponds to the natural period calculated by the microtremors.

2 - The methodology enabled a broad-scale site-response analysis to be conducted despite limited geotechnical data. Our analysis provided an indication of the level of uncertainty associated with the two geotechnical parameters soil thickness and seismic velocity, for which the amplification factors are the most sensitive. The seismic velocities are comparable with the drilling results.

3 - The soil in the study area presented different velocity structures. Three different depth levels were determined: 0-5 m, 5-15 m and 15-25 m. The seismic velocities varied between 380 and 470 m s⁻¹ for the first 5 m; 320 and 480 m s⁻¹ for 5-15 m; and 470 and 750 m s⁻¹ for 15-25 m. However, Stations 1 and 3 exhibit a similar seismic velocity structure. Station 2 exhibits different velocity characteristics due to improvements in seismic velocity values. Station 4 presents a similar soil structure along the deep profile.

4 - Our analysis determined the correlations, calculated periods and amplifications from microtremor and acceleration data. The periods were approximately identical (Fig. 8a). The shape and amplitude of the H/V spectral ratio of the microtremor for each site were similar to the shape and amplitude of the H/V spectral ratio for the seismic motion. The amplifications showed differences due to different sources of the data (Fig. 8b). This difference can be explained by the effects of the local topography. The study indicated that the alluvial soils in Antakya can significantly amplify the ground shaking associated with an earthquake. The incorporation of uncertainty revealed that a range of possible amplification factors can be expected. The method assumed that the velocity in each soil model unit can be represented by a linear gradient.

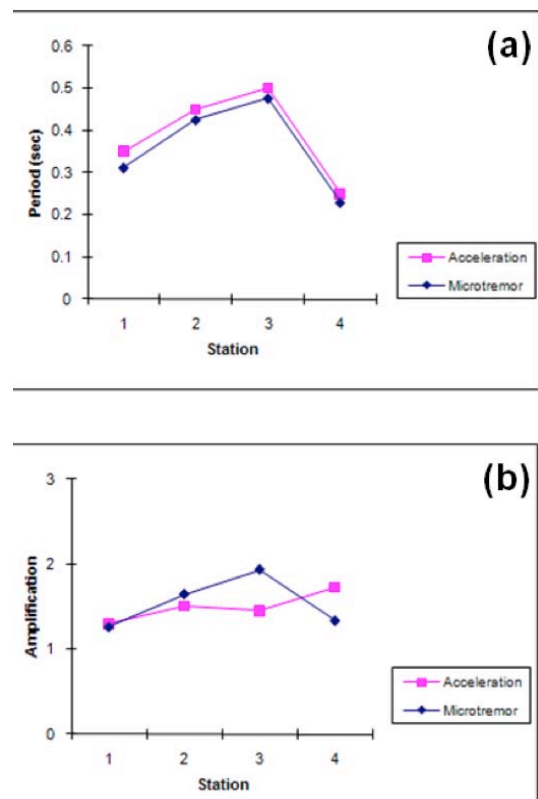


Figure 8: Comparison of acceleration and microtremor data (a) Period changes and (b) Amplification changes.

Acknowledgements

The authors are grateful to Dr.-Ing. Jochen Schwarz and Dipl.-Ing. Lars Abrahamczyk from the Earthquake Damage Analysis Center (EDAC) of Bauhaus University in Weimar, Germany for the permission to use the recorded data provided by the collaborate SERAMAR project. The instruments donated by SYSCOM Inc., Switzerland and the financial support from The Scientific and Technological Research Council of Turkey (TUBITAK) under the project Grant No. 106M420 are also appreciated. This paper has been reviewed by Dr. Hakan Cinar of Karadeniz Technical University, Turkey, which has significantly improved its quality.

References

- Abrahamczyk, L., Schwarz, J., Lang, D.H., Leipold, M., Golbs, Ch., Genes, M.C., Bikce, M., Kacin, S., and Gülkan, P. (2008). Building monitoring for seismic risk assessment (I): Instrumentation of RC frame structures as a part of the SERAMAR project. 14th World Conference on Earthquake Engineering (WCEE), Beijing 2008, China.
- Ambraseys, N.N. (1970). Some characteristic features of the Anatolian fault zone, *Tectonophysics*, 143-165.
- Ambraseys, N. N. and Barazangi, M. (1989). The 1759 earthquake in the Bekaa valley: Implications for earthquake hazard assessment in the eastern Mediterranean region, *Journal of Geophysical Research*, 94 (B4), 4007-4013.
- Ambraseys, N.N., Jackson, J.A. (1998). Faulting associated with historical and recent earthquakes in the Eastern Mediterranean region, *Geophysical Journal International*, 133, 390-406.
- Clough, R. and Penzien, J. (1993). *Dynamics of structures*. New York: McGraw Hill
- EDAC (2004). Turkish-German-Swiss Joint Project on Seismic Risk Assessment and Mitigation in the Antakya-Maraş Region on the basis of Microzonation, Vulnerability and Preparedness Studies (SERAMAR)-Project description. Earthquake Damage Analysis Center, Bauhaus-Universität Weimar, October 2004.
- Erdik, M., Aydınoglu, N., Kalafat, D. and Pinar, A. (1997). January 22, 1997 (Mw=5.8) Antakya, Turkey. Earthquake International Association of Seismology and Physics of the Earth's Interior (IASPEI), Thessaloniki, Greece, August 1997, 17-28.
- Ergin, K., Guclu, U., Uz, Z. (1967). A catalogue of earthquakes of Turkey and surrounding area (11 AD to 1964 AD). Maden Fakültesi, Arz Fizigi Enstitüsü Yayınları, İstanbul, 24, 1-28.
- Jackson, J. A. and McKenzie, D. (1988). The relationship between plate motions and seismic moment tensors, and the rates of active deformation in the Mediterranean and Middle East, *Geophys. J. R. Astr. Soc.*, 93, 45-73.
- Kalafat, D. and Bagci, G. (2001). Adana ve Doğu Anadolu fay zonunun depremsellik özellikleri. TMMOB, Jeofizik Mühendisleri toplantısı-Adana, 36-43.
- Kanai, K. (1957). The requisite conditions for predominant vibration of ground. *Bulletin of Earthquake Research Institute, University of Tokyo*, 35, 457.
- Lyberis, N., Yurur, T., Chorowicz, J., Kasapoglu, E. and Gundogdu, N. (1992). The East Anatolian fault: an oblique collisional belt. *Tectonophysics*, 204, 1-15.
- McKenzie, D. (1978). Some remarks on the development of sedimentary basins, *Earth and Planet Sci. Lett.*, (40), 25-32.
- McKenzie, D. (1972). Active Tectonics of the Mediterranean Region, *Geophysical Journal of the Royal Astronomical Society*, 30(2), 109-185.
- Mohraz, B., Elghadamsi, F.E. (1989). *The seismic design handbook*. New York: Van Nostrand Reinhold.
- Over, S., Büyüksaraç, A., Bektaş, O. and Filazi, A. (2011). Assessment of potential seismic hazard and site effect in Antakya (Hatay Province), SE Turkey. *Environmental Earth Sciences*, 62, 313-326.
- Over, S., Büyüksaraç, A., Bektaş, O., Arisoy, M. O. and Filazi, A. (2008). Hatay İli Merkezinin (Antakya) Deprem Duyarlık ve Mikrobölgeleme Projesi, Mustafa Kemal University (Internal Project, in Turkish).
- Over, S., Ozden, S. and Yılmaz, H. (2004a). Late Cenozoic stress evolution along the Karasu Valley, SE Turkey. *Tectonophysics*, 380, 43-68.
- Over, S., Unlugenc, U.C. and Bellier, O. (2002). Quaternary stress regime change in the Hatay region (SE Turkey). *Geophysical Journal International*, 148, 1-14.
- Perincek, D. and Eren, A.G. (1990). Doğrultu atımlı Doğu Anadolu ve Olu Deniz fay zonları etki alanında gelişen Amik havzasının kökeni. Türkiye 8. Petrol Kongresi Bildiri Kitabı, 180-192.
- Poirier, J.P. and Taher, M.A. (1980). Historical seismicity in the near and Middle East, North Africa, and Spain from Arabic documents (VIIth-XVIIIth Century), *Bulletin of the Seismological Society of America*, 70(6), 2185-2201.
- Robinson, D., Dhu, T. and Schneider, J. (2006). SUA: A computer program to compute regolith site-response and estimate uncertainty for probabilistic seismic hazard analyses, *Computers & Geosciences*, 32, 109-123.
- Rojay, B., Heimann, A. and Toprak, V. (2001). Neotectonic and volcanic characteristics of the Karasu Fault zone (Anatolia, Turkey): The transition zone between the Dead Sea transform and the East Anatolian fault zone. *Geodinamica Acta*, 14, 197-212.
- Rotstein, Y. and Kafka, A. L. (1982). Seismotectonics of the southern boundary of Anatolia, eastern Mediterranean region: Subduction, collision, and arc jumping, *Journal of Geophysical Research*, 87(B9), 7694-7706.
- Schwarz, J., Abrahamczyk, L., Langhammer, T., Leipold, M., Genes, M.C., Bikce, M. and Kacin, S. (2009). Building typology for risk assessment: case study Antakya (Hatay). Earthquake and Tsunami, İstanbul, Turkey.
- Schwarz, J., Lang, D.H., Abrahamczyk, L., Bikce, M., Genes, M.C. and Kacin, S. (2007). Seismische Instrumentierung Mehrgeschossiger Stahlbetonbauwerke-ein Beitrag Zum SERAMAR Project. Der Österreichischen Gesellschaft Für Erdbebeningenieurwesen und Baudynamik (D-A-CH TAGUNG 2007), 28 September 2007, Wien.
- Shrikhande, M. and Basu, S. (2004). Strong motion v/s weak motion: Implications for seismic microzonation. *Journal of Earthquake Engineering*, 8, 159-173.
- Soysal, H., Sipahioglu, S., Kolcak, D. and Altinok, Y. (1981). Türkiye tarihsel deprem katalogu. TUBITAK Project (No: TBAG-341), Ankara.
- Tehrani-zadeh, M. and Hamed, F. (2002). *Engineering Structures*, 24, 933-943.
- Udwadia, F.E. and Trifunac, M.D. (1973). Comparison of earthquake and microtremor ground motion in El Centro, California. *Bulletin of the Seismological Society of America*, 63, 1227-1253.
- Westaway, R. (1994). Present-day kinematics of the Middle East and eastern Mediterranean. *Journal of Geophysical Research*, 99 (B6), 12071-12090.